Some case studies

The adiabatic model predicts with good accuracy the main reaction channels (or reaction windows) for electron capture of Type 1 by multiply charged ions from atoms such as H or He. Experiments on ion-atom systems, confirm these predictions (although there are some discrepancies between theory and experiment for the absolute cross section values.

If type I reactions are not energetically favoured, then type II reactions can become important. Type II reactions involve configuration mixing of the electrons of the collision complex. The electron capture process is accompanied either by an excitation of the ion core or by an excitation of the target electrons.

For an H target, type II reactions only occur for doubly or trebly open shell ions. But for other targets (in particular molecular targets) excitation of the target may occur and a large variety of reactions may occur. For molecular targets , electron capture often leads to dissociation.

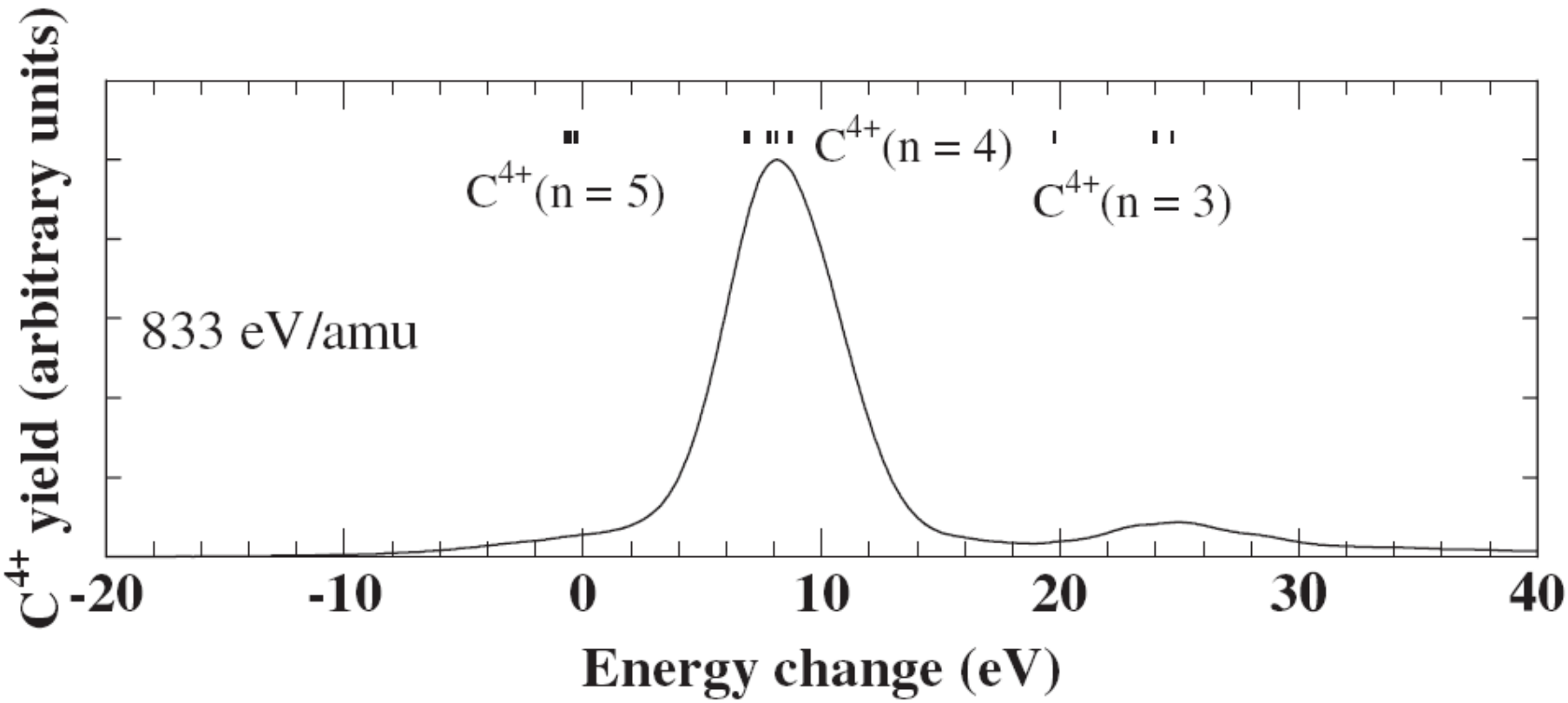

Energy-change spectrum for one-electron capture by C^{5+} ions in H at 833 eV amu^{-1}.

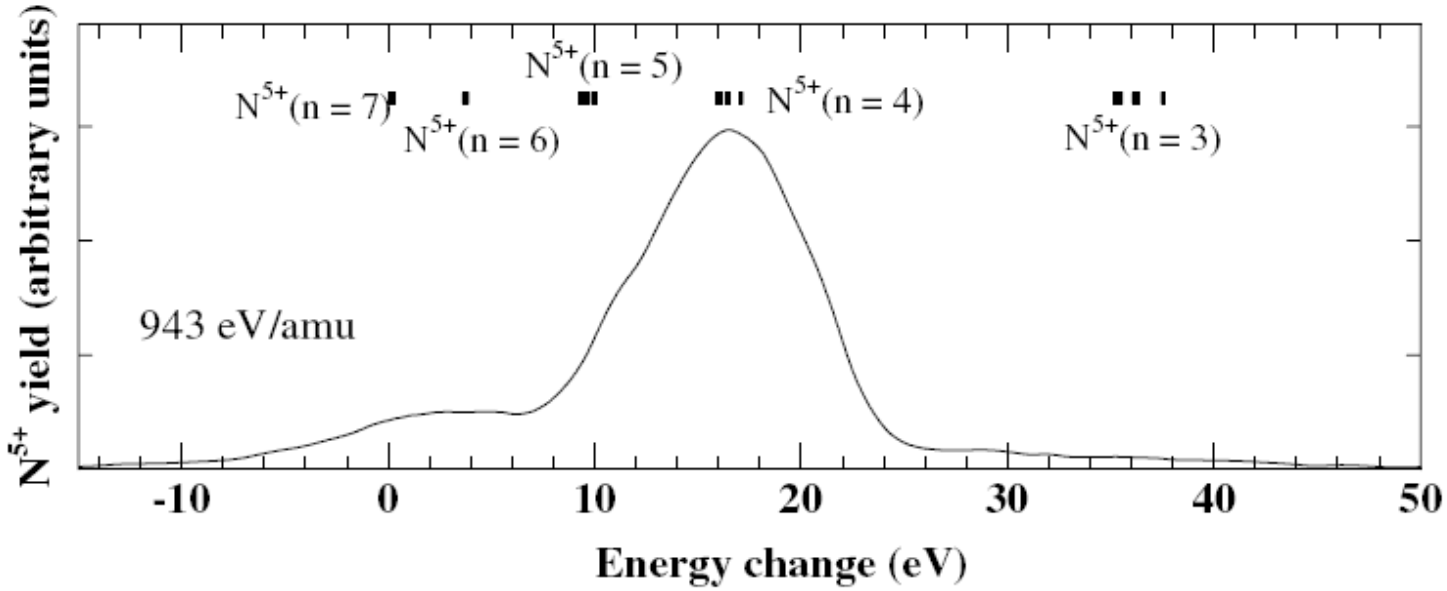

Energy-change spectrum for one-electron capture by N^{6+} ions in H at 943 eV amu^{-1}.

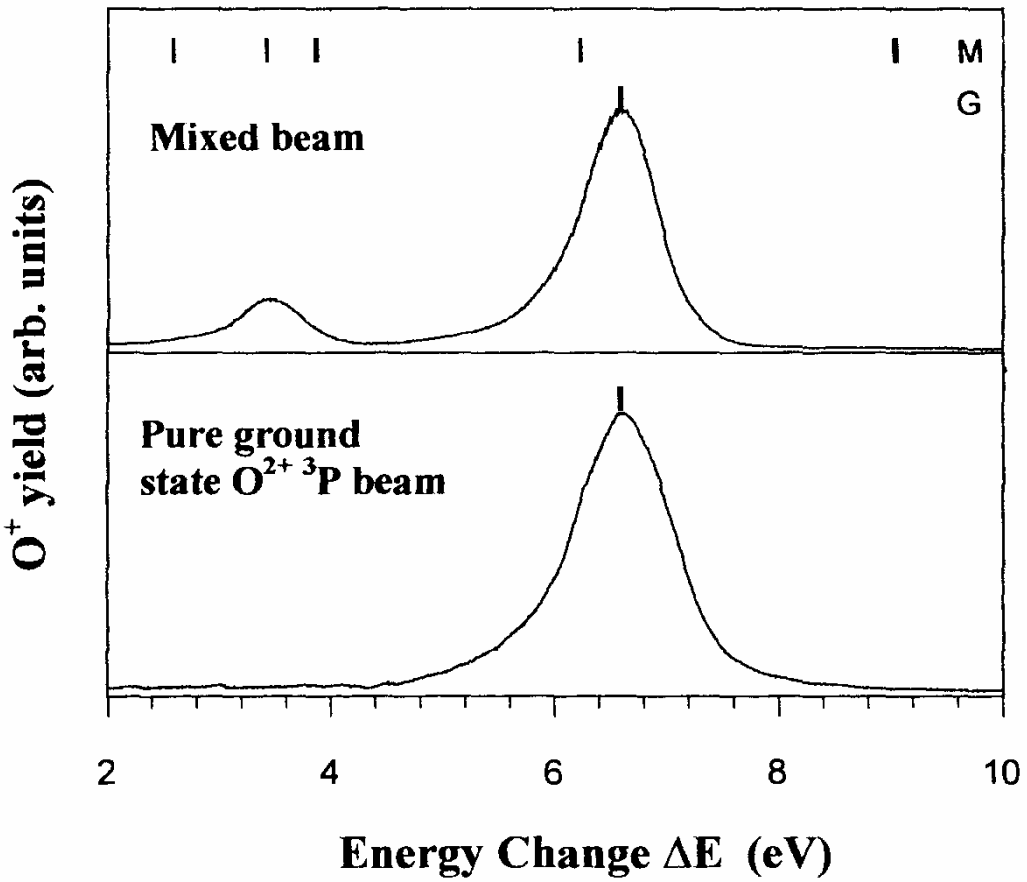

Energy spectra for one electron capture in O^{2+}/H collisions (a) by a beam of O^{2+} of unknown metastable content and (b) by a pure O^{2+} source.

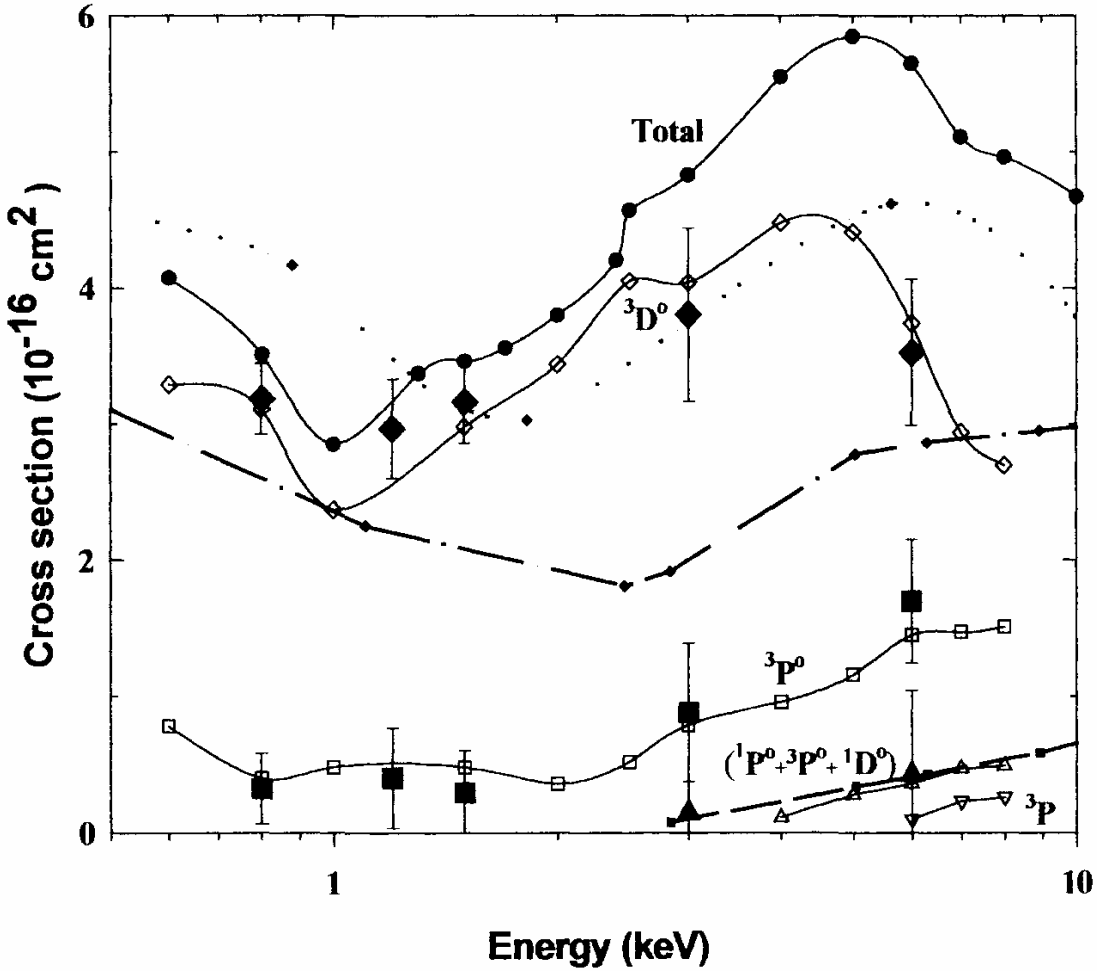

Figure 10.14. Cross sections for one-electron capture by N^{2+} ions in atomic hydrogen leading to specified N^+ (n, l) products. DTES measurements [31] with pure ground-state N^{2+} $^2P^o$ ions, ♦, $^3D^o$; ■, $^3P^o$; ▲, ($^1D^o$ + $^1P^o$+ $^3P^o$). Previous TES measurements [44] using an N^{2+} beam containing an unknown fraction of metastable ions, •, total; ◊, $^3D^o$; □, $^3P^o$; △, ($^3P^o$ + $^1P^o$ + $^1D^o$); ▽, ^3P. Theory [47], · · · · · · · ·, $^3D^o$. *Theory* [49], — · — ·, $^3D^o$; — — —, $^3P^o$.

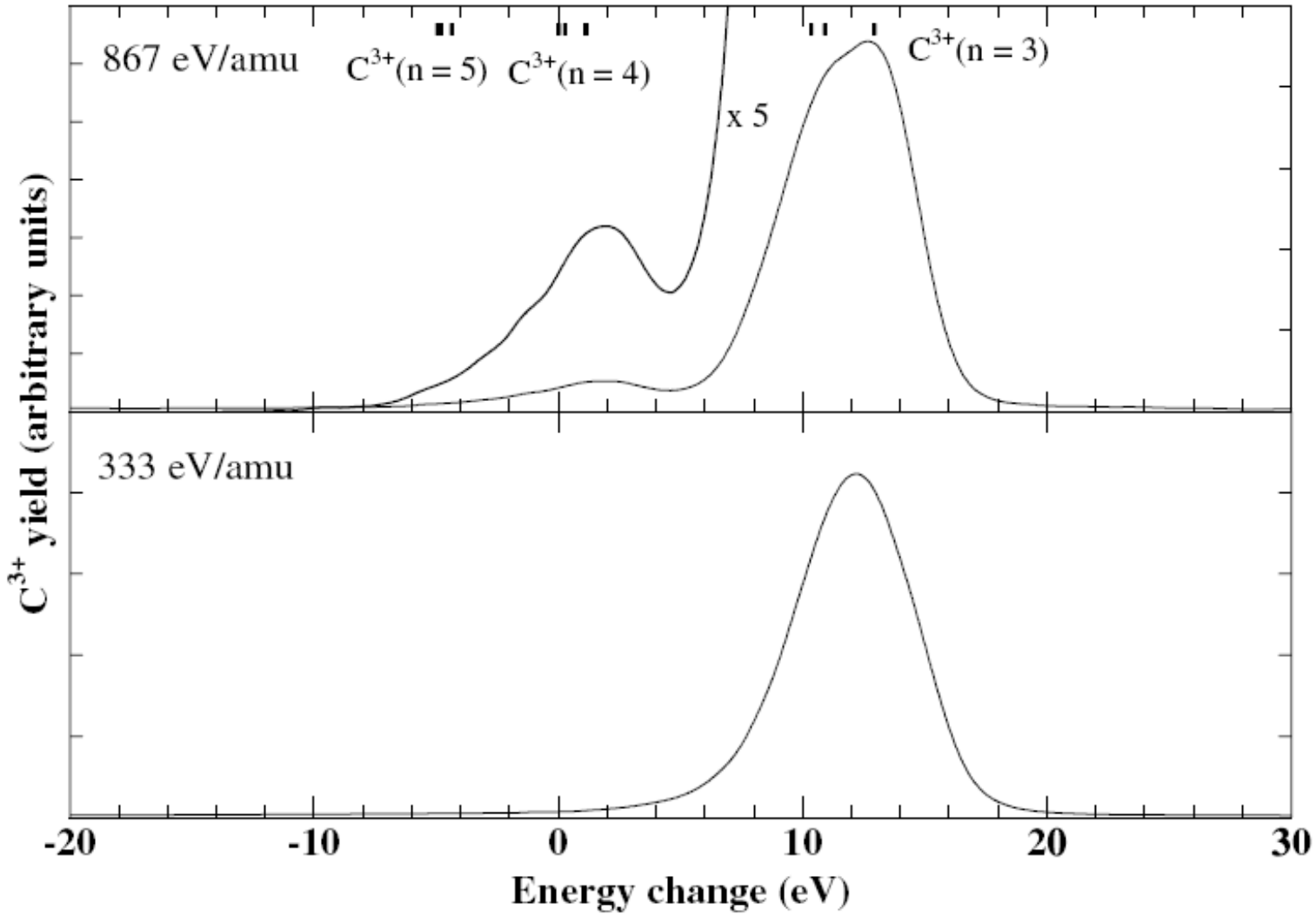

Figure 8. Energy-change spectra for one-electron capture by C^{4+} ions in H at 867 and 333 eV amu^{-1}.

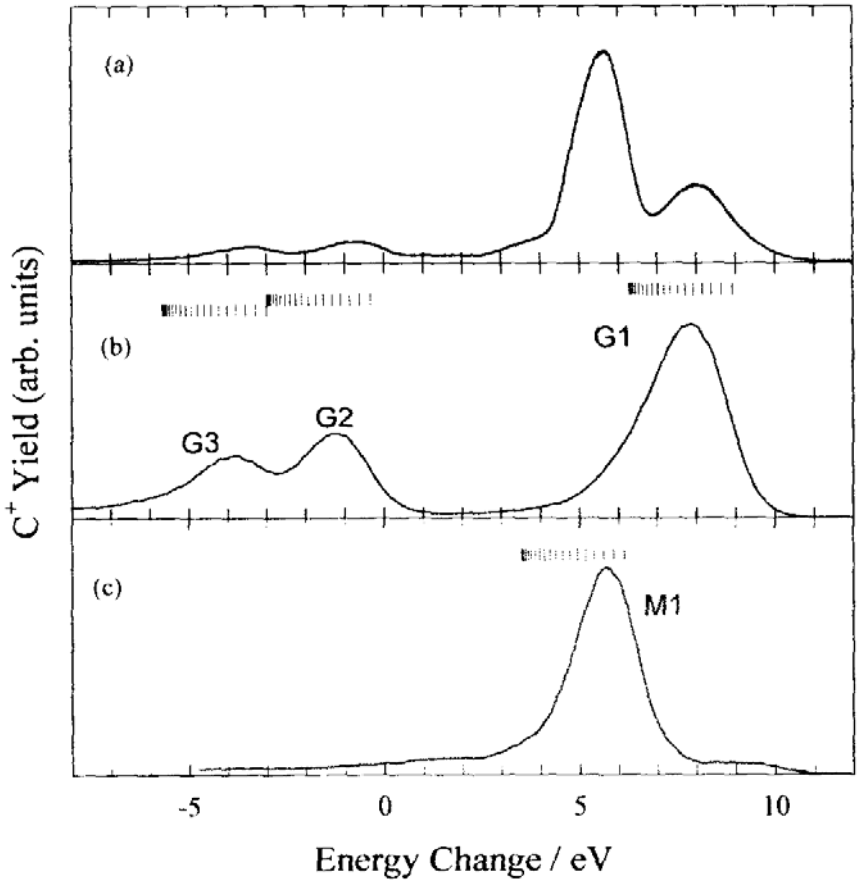

Energy spectra for electron capture in C^{2+} /H_2 collisions at 500eV/amu by (a) a mixed beam of ground and metastable C^{2+}, (b) a pure ground state beam of C^{2+} ions and (c) a pure metastable beam

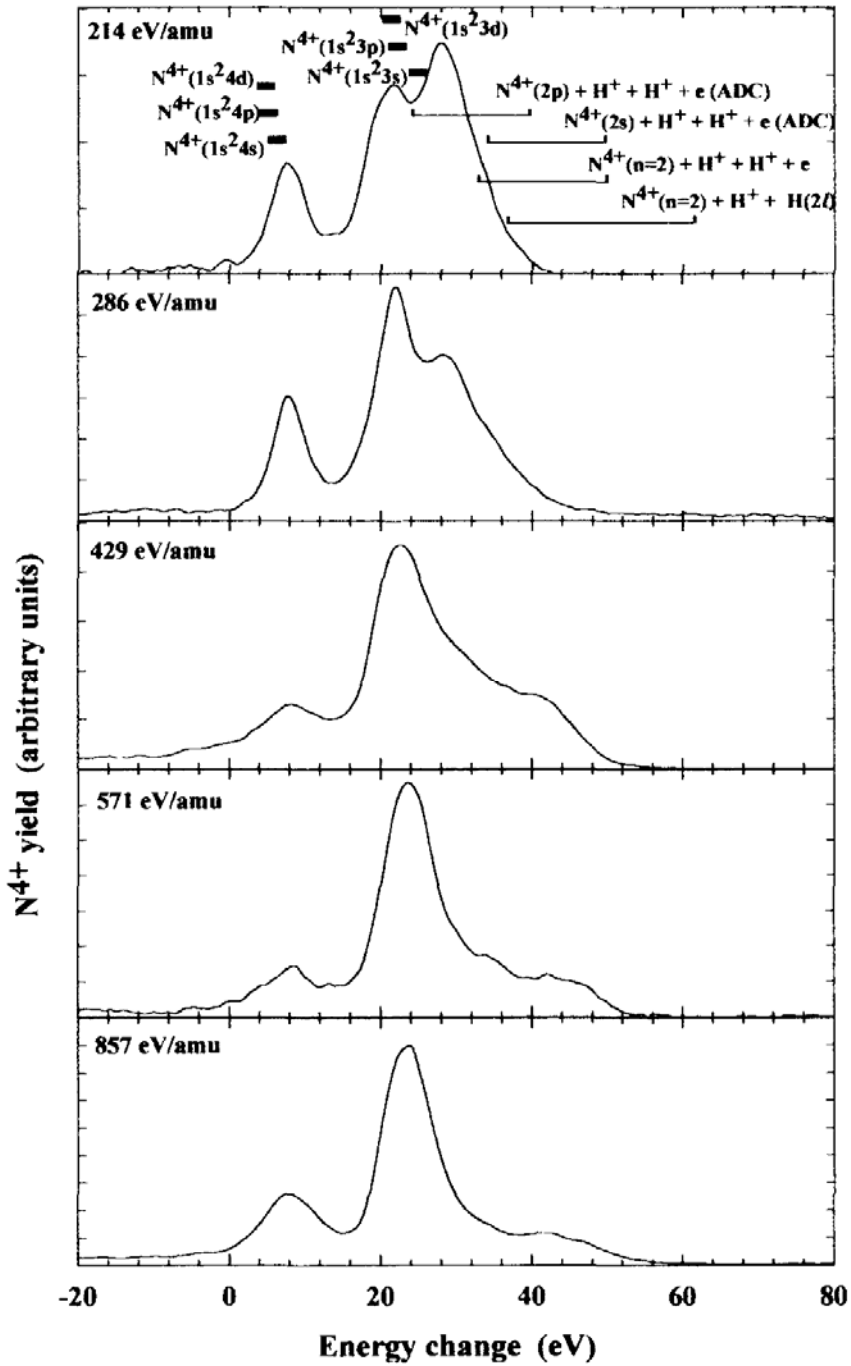

Interesting case of N^{2+} - H_2 collisions

Non dissociative capture.

Dominant process

$N^{5+} + H_2 \rightarrow N^{4+} (1s^2\ 3s, 3p, 3d) + H_2^+$

Secondary

$N^{5+} + H_2 \rightarrow N^{4+} (1s^2\ 4s, 4p, 4d, 4f) + H_2^+$

Dissociative capture

Main process

$N^{5+} + H_2 \rightarrow N^{4+} (n=2) + H^+ + H(2l)$

Secondary

$N^{5+} + H_2 \rightarrow N^{4+} (n=2) + H^+ + H^+ + e$

Table 1. Summary of the extent to which calculated reaction windows correctly describe observed energy-change spectra in one-electron capture by slow He and H-like ions of O, N and C in collisions with H and H_2.

Process	Impact energy (eV amu^{-1})	ΔE (eV) corresponding to the peak of the calculated reaction window	Comments
$O^{6+} + H_2$	900	16.0	Reaction window correctly accommodates most of the captures corresponding to the dominant O^{5+} ($n = 4$) peak
$N^{5+} + H_2$	857	17.0	Reaction window fails to accommodate the main peaks corresponding to N^{4+} ($n = 4$) and N^{4+} ($n = 3$) formation
$C^{4+} + H_2$	867	10.3	Reaction window correctly predicts the dominance of C^{3+} ($n = 3$) products
$O^{7+} + H_2$	875	18.5	Reaction window falls between the two main O^{6+} ($n = 4$) and O^{6+} ($n = 5$) product peaks
$N^{6+} + H_2$	943	16.0	Reaction window correctly predicts the dominance of N^{5+} ($n = 4$) products
$C^{5+} + H_2$	833	11.4	Reaction window falls between the two main C^{4+} ($n = 4$) and C^{4+} ($n = 3$) product peaks
$O^{6+} + H$	900	14.5	Reaction window correctly accommodates most of the captures corresponding to the dominant O^{5+} ($n = 4$) peak
$N^{5+} + H$	857	16.5	Reaction window falls between the N^{4+} ($n = 4$) and N^{4+} ($n = 3$) product peaks but correctly favours the former
$C^{4+} + H$	867	10.4	Reaction window correctly accommodates most of the captures corresponding to the dominant C^{3+} ($n = 3$) peak
$O^{7+} + H$	875	15.0	Reaction window correctly accommodates most of the captures corresponding to the dominant O^{6+} ($n = 5$) peak
$N^{6+} + H$	943	14.3	Reaction window correctly accommodates most of the captures corresponding to the dominant N^{5+} ($n = 4$) peak
$C^{5+} + H$	343	13.0	Reaction window falls between C^{4+} ($n = 4$) and C^{4+} ($n = 3$) product peaks but correctly favours the former

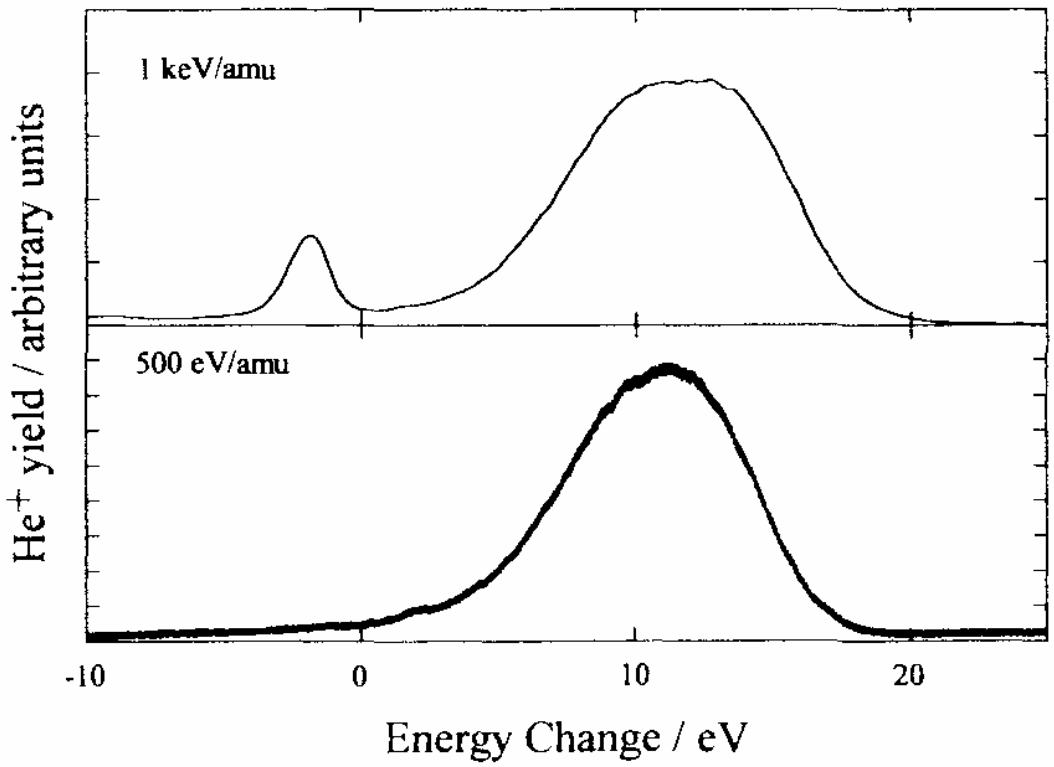

Energy spectra for He^{2+} ions in H_2 . 3 Main product channels

$He^{+}(n=2)+ H_2^{+}$ -1.79—4.44 eV endothermic

$He^{+}(1s)+H^{+} +H(2s)$ 4.30 -18.36 eV exothermic

He+(1s)+H+ +H(2p) 4.40 – 12.73 eV exothermic

At low energies dissociative electron capture dominates.

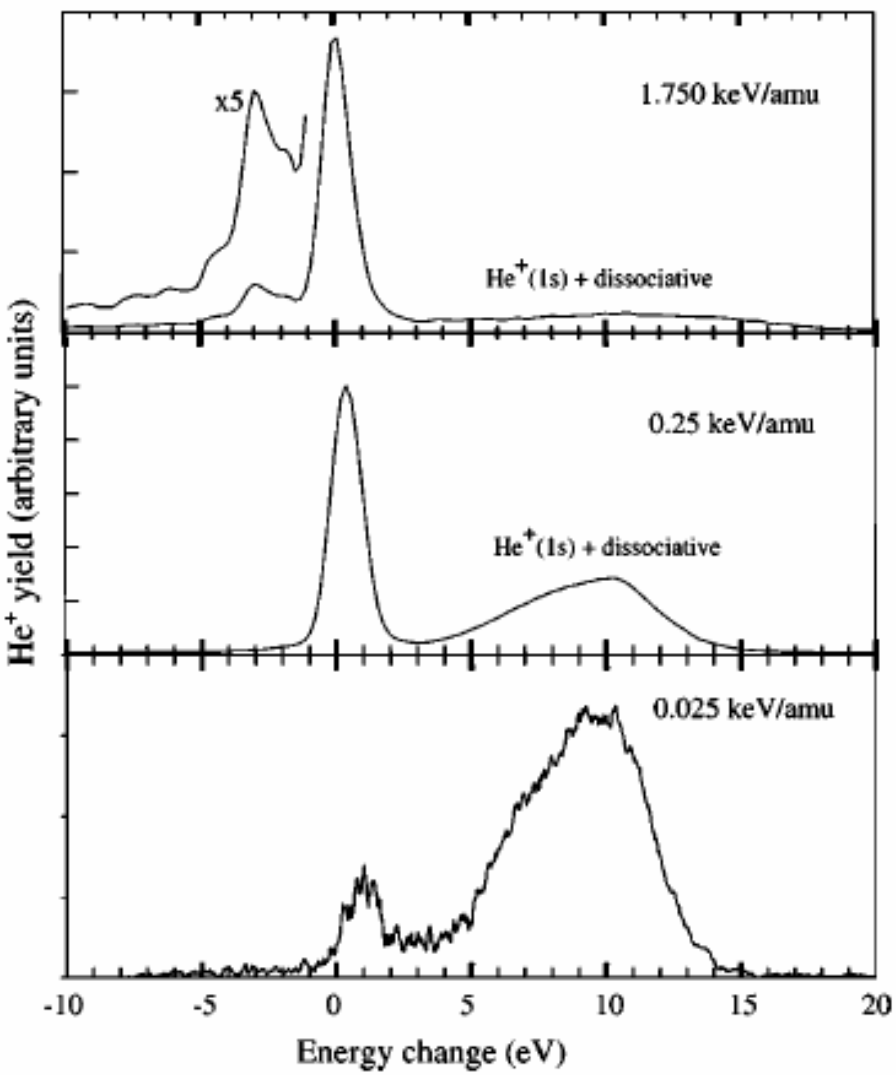

FIG. 1. Energy change spectra for one electron capture by He^{2+} ions in H_2O at three representative energies recorded by the QUB and WMU translational energy spectrometers ssee textd.

TABLE I. Product channels and corresponding energy defects for one-electron capture by He^{2+} ions in H_2O.

Product channels	Energy defects (eV)
$He^+\ (n=3)+H_2O^+[\tilde{A}^2A_1]$	−7.79–−10.61
$He^+\ (n=3)+H_2O^+[\tilde{X}^2B_1]$	−6.57–−7.35
$He^+\ (n=2)+H_2O^+[\tilde{B}^2B_2]\Rightarrow OH^+, O^+, H^+$	−4.50–−5.11
$He^+\ (n=3)+H_2O^+[\tilde{B}^2B_2]$	−3.57–−6.39
$He^+\ (n=2)+H_2O^+[\tilde{A}^2A_1]$	−0.23–−3.05
$He^+\ (n=2)+H_2O^+[\tilde{X}^2B_1]$	0.20–0.98
$He^+\ (n=1)+H_2O^{2+}[^3B_1]+e$	17.90
$He^+\ (n=1)+H_2O^{2+}[^1A, ^1B]+e$	12.40–14.40
$He^+\ (n=1)+H_2O^{2+}[(2)^1A_1]+e$	9.10

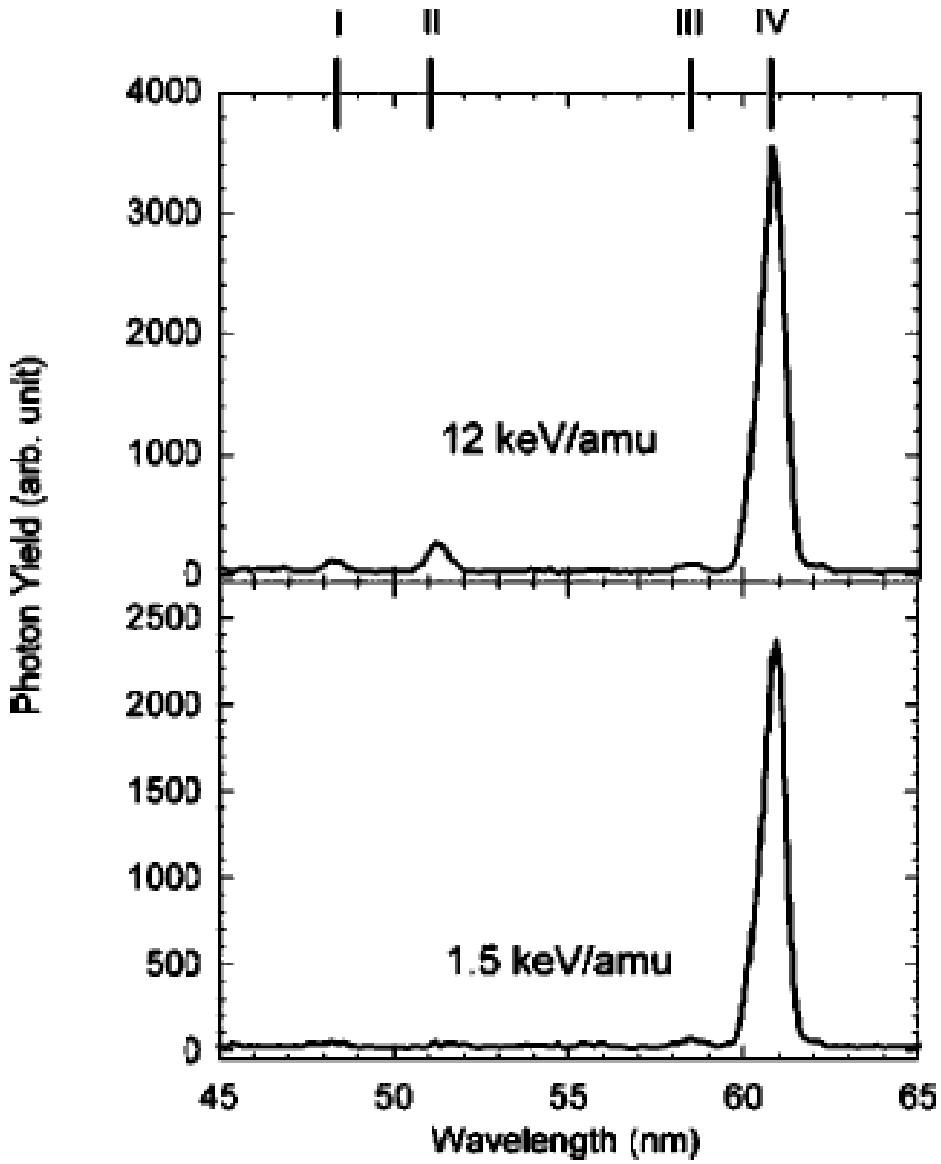

FIG. 2. Photon emission spectra for one-electron capture in $He^{2+}-H_2O$ collisions observed at two different velocities. The following emission features are indicated: I—second order of He II (4*p*-1*s*) at 24.3 nm; II—second order of He II (3*p*-1*s*) at 25.6 nm; III—He I (1*s*2*p*-1*s*2) at 58.4 nm; IV—second order of He II (2*p*-1*s*) at 30.4 nm.

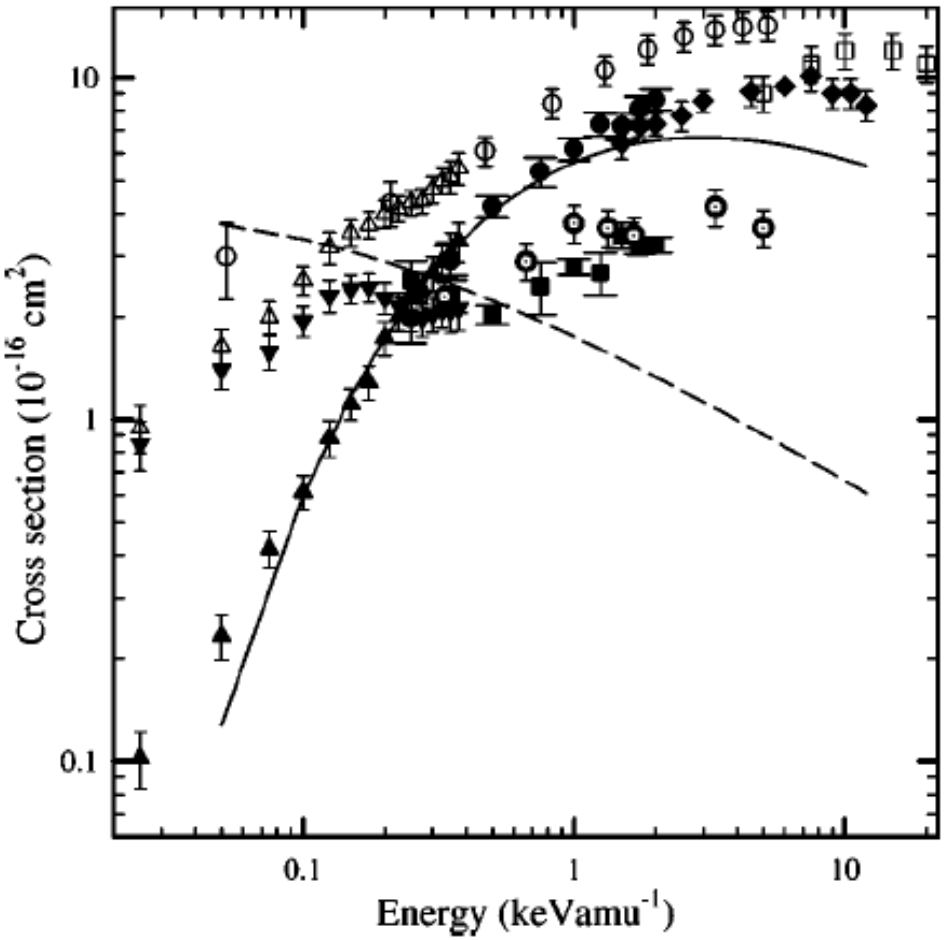

FIG. 5. Cross sections for one electron capture by He^{2+} ions in H_2O. Total cross sections: open squares, Rudd *et al.* [6]; open circles, Greenwood *et al.* [9]; open triangles, present work. Capture into He^+ ($n=2$) states: closed circles, QUB; closed triangles, WMU. He II ($2p$-$1s$): closed diamonds, KVI. Capture into He^+ ($n=1$) state: closed squares, QUB; inverted triangles, WMU. Transfer ionization: circles with cross hairs, HMI. Theory: solid line, He^+ ($n=2$) formation; dashed line, He^+ ($n=1$) formation.

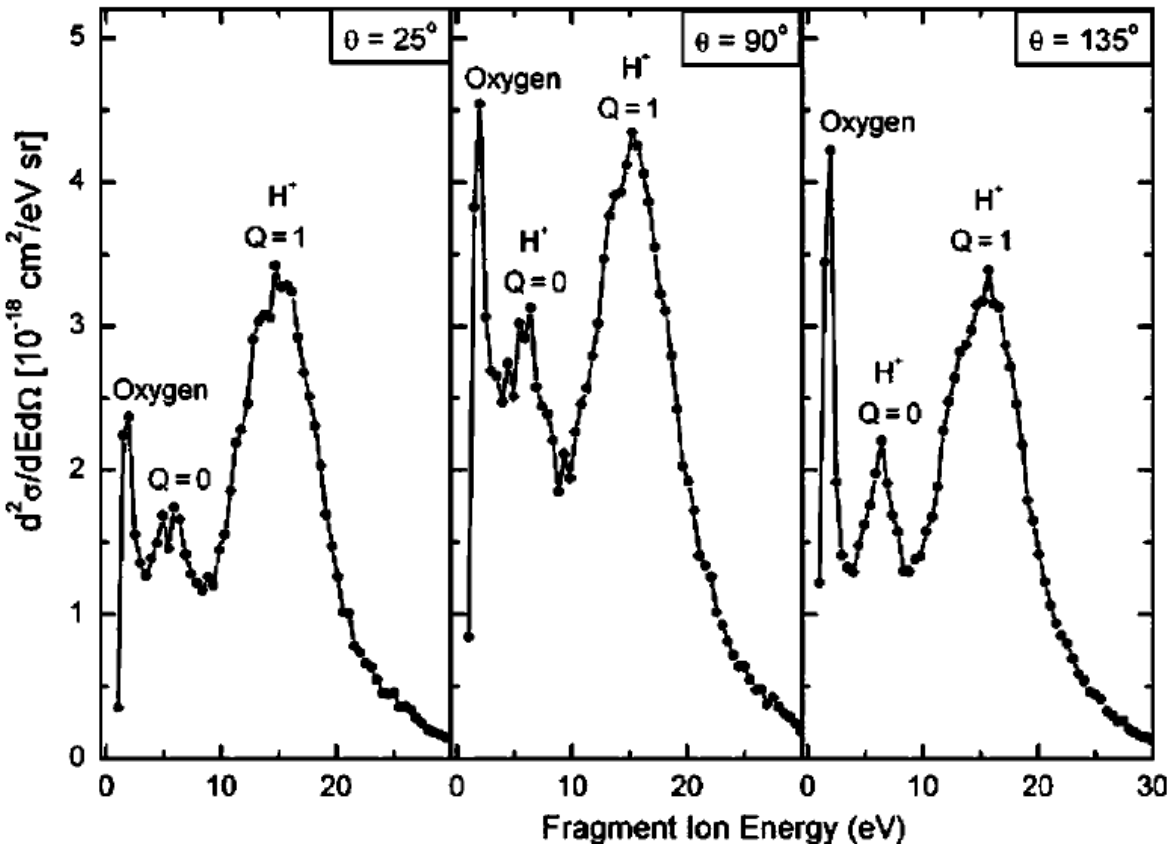

FIG. 3. Energy spectra of fragment ions from the interaction of 4-kev He^{2+} ions with H_2O molecules. The observed fragments are formed exclusively in large impact parameter collisions. The observation angles were $\Theta = 25°$, 90°, and 135°.

Peak labeled oxygen: $H_2O^{2+} \rightarrow \underline{O^+} + H^+ + H^0$ and

$\rightarrow \underline{OH^+} + H^+$,

Peak labeled $Q = 0$: $H_2O^{2+} \rightarrow O^0 + \underline{H^+} + H^+$,

Peak labeled $Q = 1$: $H_2O^{2+} \rightarrow OH^+ + \underline{H^+}$ and

$\rightarrow O^+ + H^+ + H^0$.

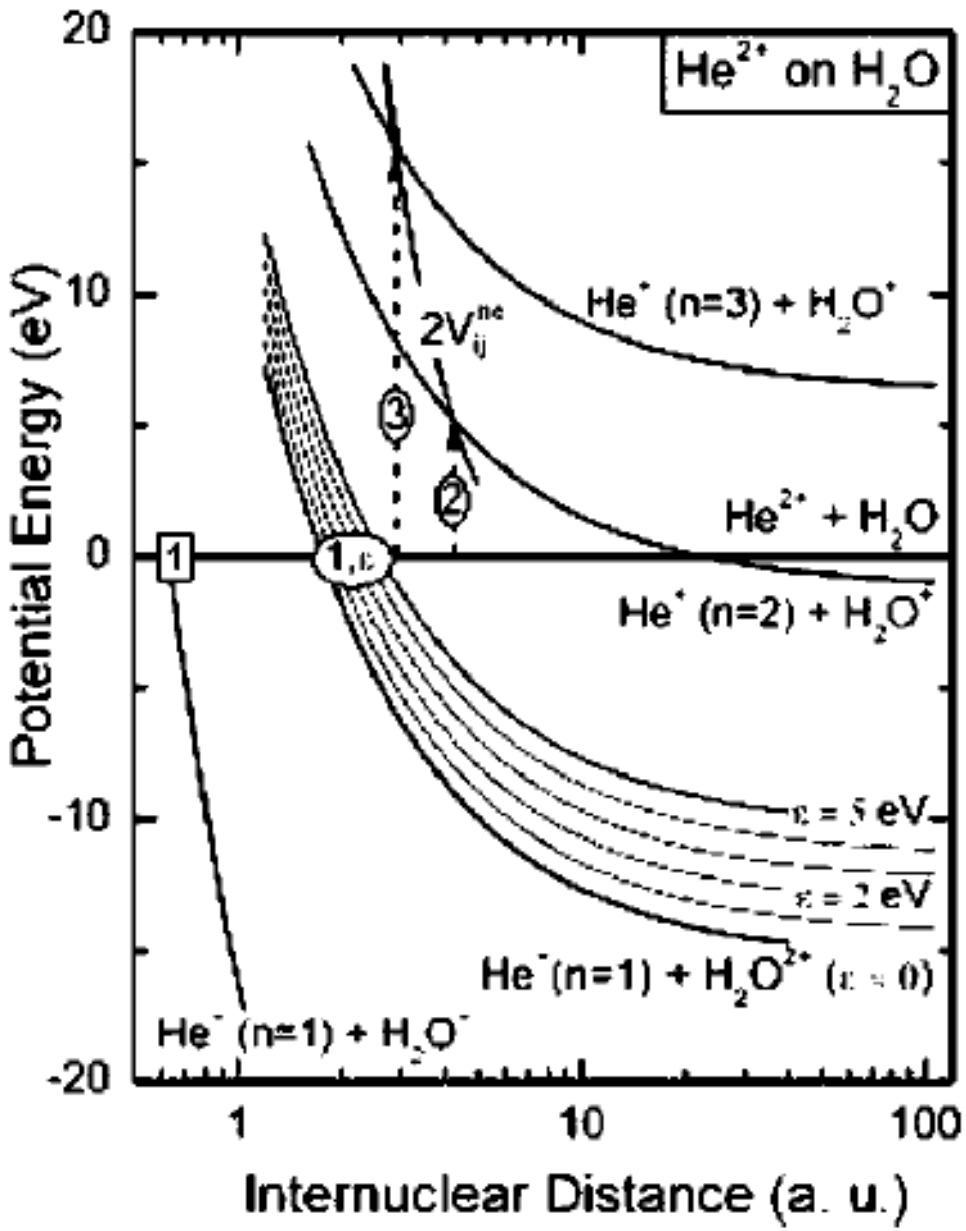

FIG. 4. Potential curves for the He^{2+}-H_2O system. Single-electron transitions populating the *n*=1, 2, and 3 states of He+ are denoted by 1, 2, and 3, respectively. Dielectronic transitions populating the *n*=1 state and the continuum state ε are denoted (1,ε).

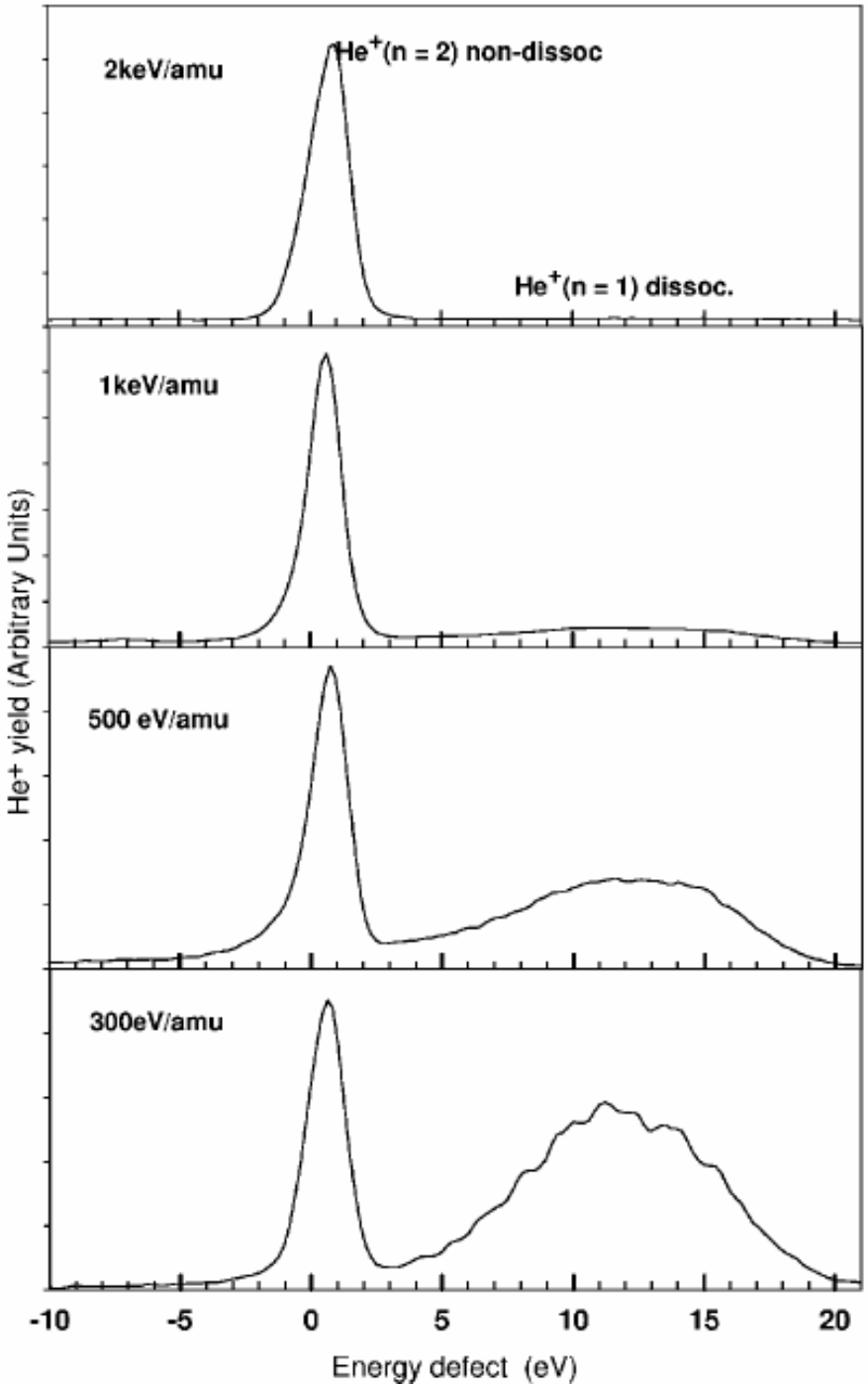

FIG. 1. Energy change spectra for one-electron capture by 300–2000 eV amu−1 He^{2+} ions in CH_4.

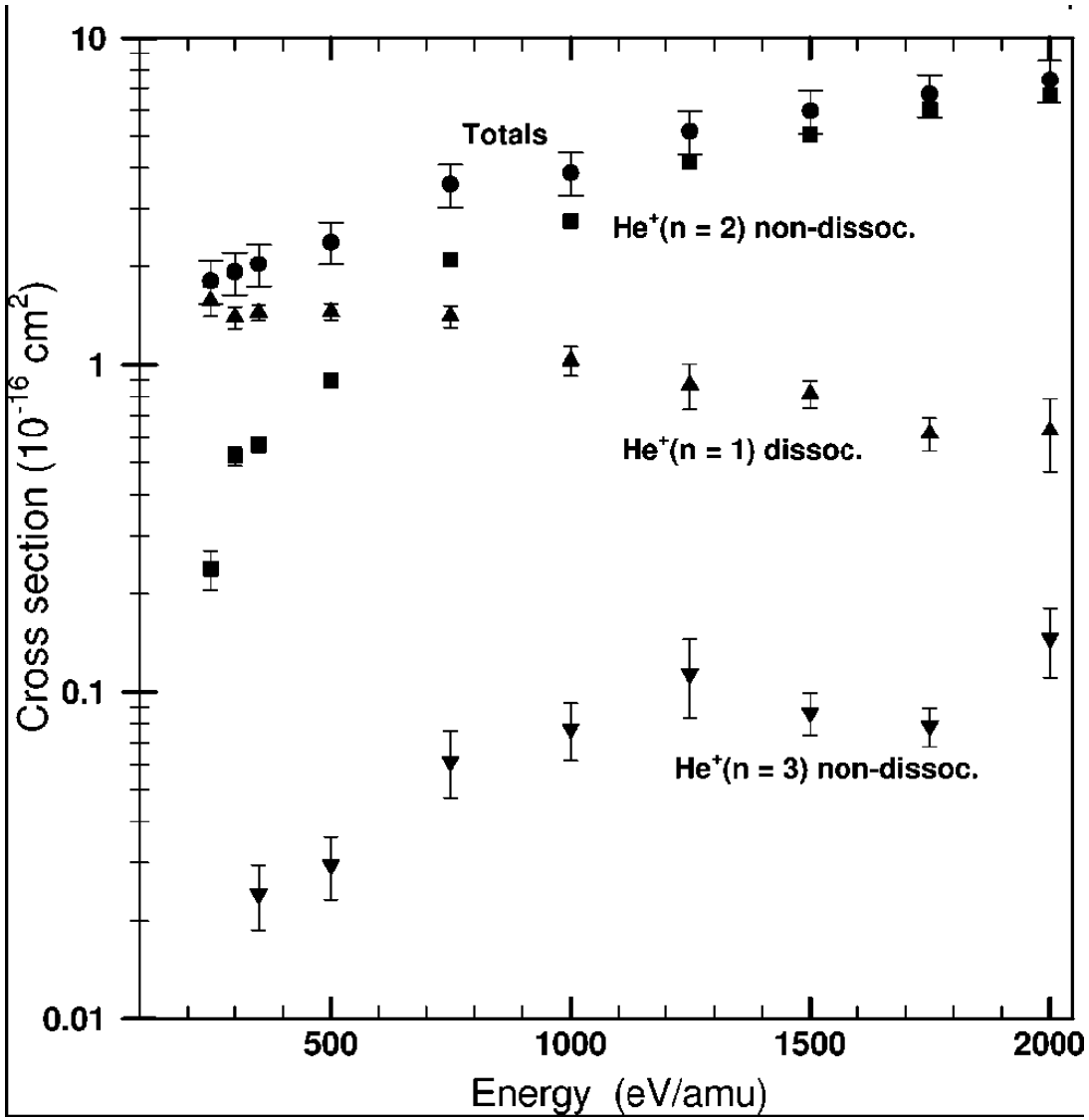

FIG. 2. Measured cross sections for main product states of He+ formed in one-electron capture by 300–2000 eV amu−1 He^{2+} ions in CH_4 together with total one-electron capture cross sections.

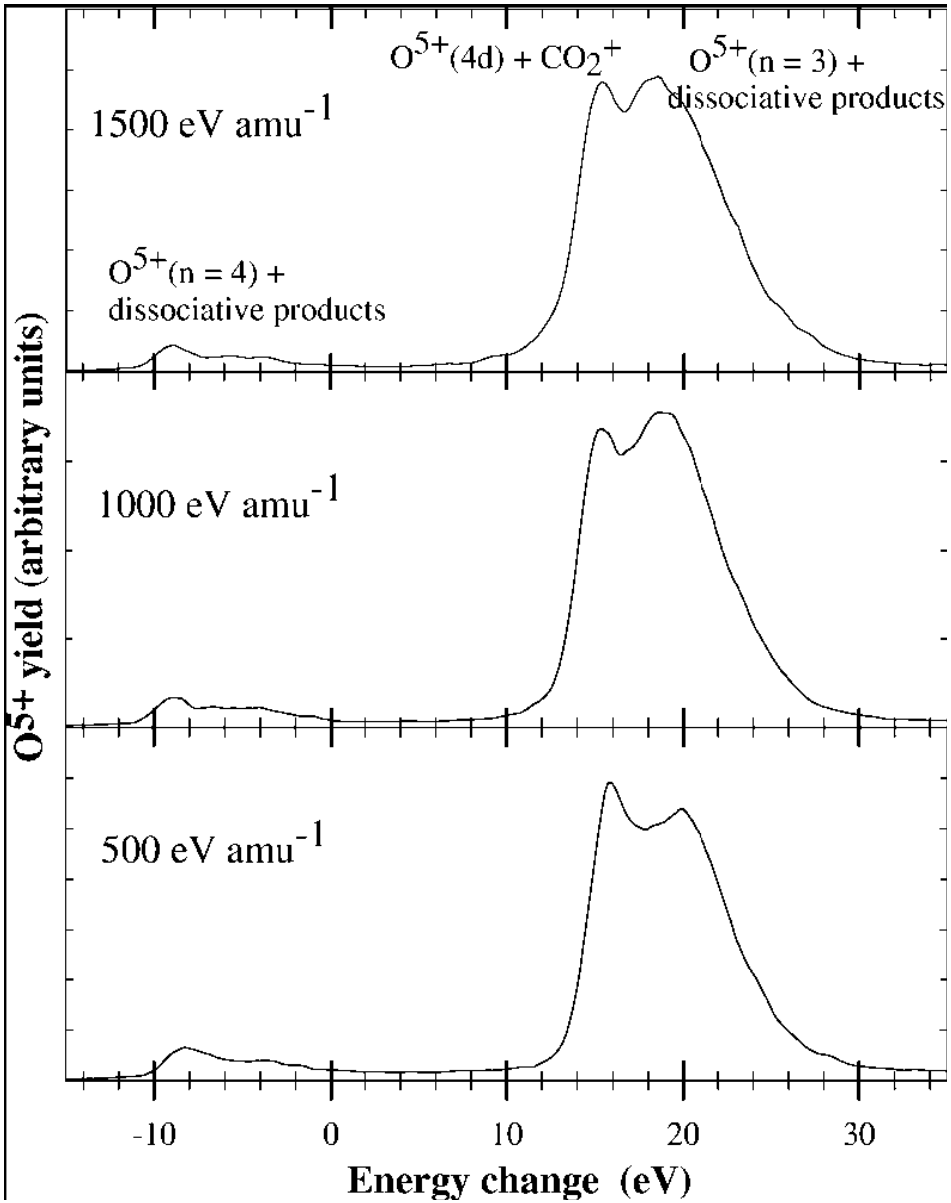

FIG. 2. Energy change spectra for one-electron capture by 500–1500 eV amu^{-1} O^{6+} ions in CO_2.

Main exit channels.

Most prominent chanel is one-electron capture to 4d state

$$O^{6+}(1s^2)^1S + CO_2[X^1\Sigma_g^+] \rightarrow O^{5+}(1s^24d) + CO_2^+[X^2\Pi_g] + (16 - 16.9)\ \text{eV}.$$

Dissociative transfer ionization

$$O^{6+}(1s^2)^1S + CO_2[X^1\Sigma_g^+] \rightarrow O^{5+}(n = 3) + (CO_2^{2+} \Rightarrow O^+, CO^+) + (16.9 - 25.7)\ \text{eV}$$

Dissociative electron capture

$$O^{6+}(1s^2)^1S + CO_2[X^1\Sigma_g^+] \rightarrow O^{5+}(n = 3) + \{CO_2^+ \Rightarrow (CO^+, O); (O^+, CO)\} + (26 - 31.8)\ \text{eV}.$$

Endothermic dissociative electron capture

$$O^{6+}(1s^2)^1S + CO_2[X^1\Sigma_g^+] \rightarrow O^{5+}(n = 4) + \{CO_2^{2+} \Rightarrow (O^+, CO^+); (C^+, O^+, O)\} - (5.0 - 10.8)\ \text{eV}.$$

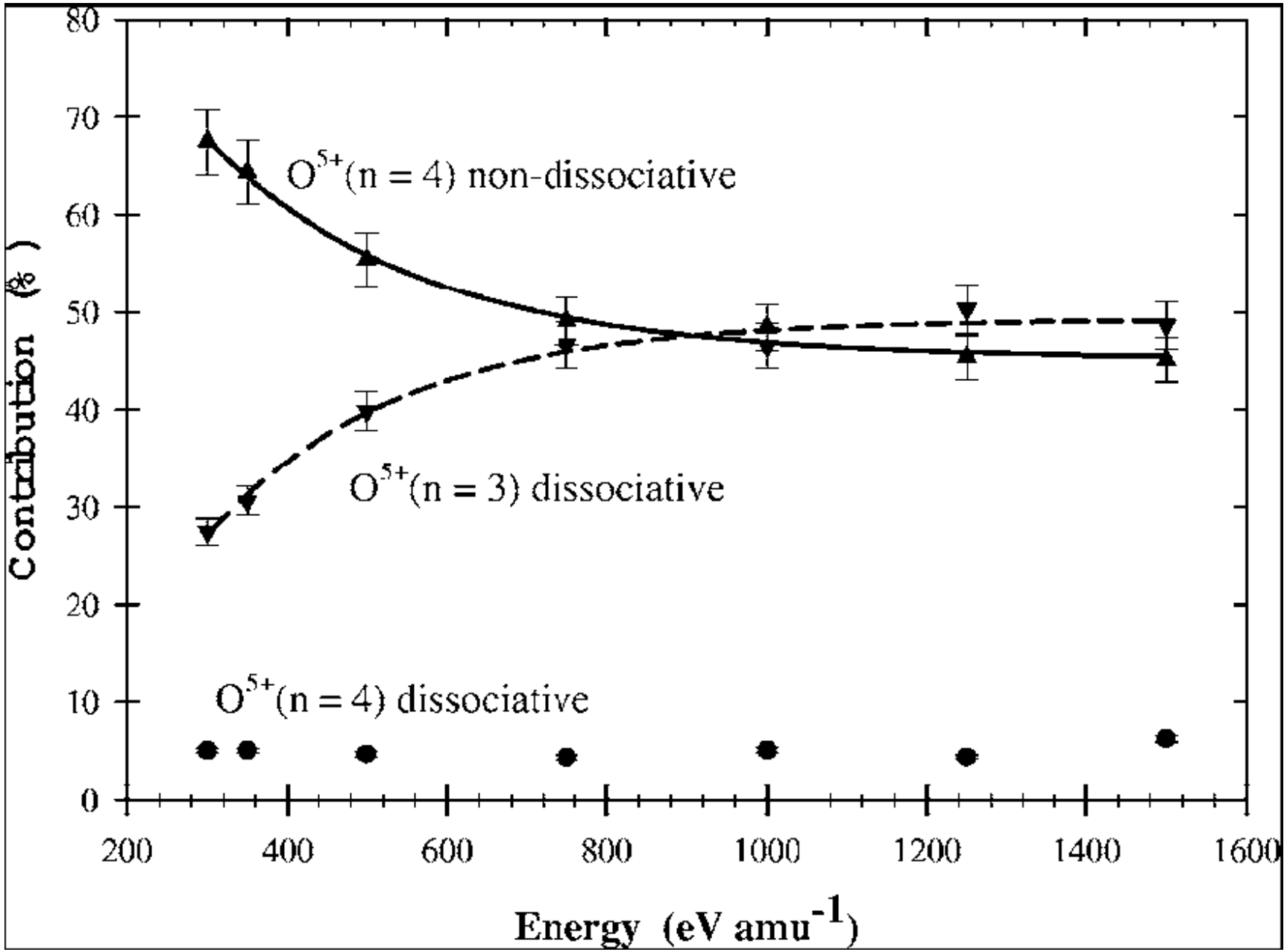
80
70
60
50
40
30
20
10
0
Contribution (%)
O5+(n = 4) non-dissociative
O5+(n = 3) dissociative
O5+(n = 4) dissociative
200
400
600
800
1000
1200
1400
1600
Energy (eV amu-1)